EUROFUSION WP15ER-PR(16) 14986

BF McMillan et al.

A partially mesh-free scheme for representing anisotropic spatial variations along field lines

Preprint of Paper to be submitted for publication in
Computer Physics Communications

This work has been carried out within the framework of the EUROfusion Consortium and has received funding from the Euratom research and training programme 2014-2018 under grant agreement No 633053. The views and opinions expressed herein do not necessarily reflect those of the European Commission.

A partially mesh-free scheme for representing anisotropic spatial variations along field lines

Ben F McMillan

(Dated: January 15, 2016)

A common numerical task is to represent functions which are highly spatially anisotropic, and to solve differential equations related to these functions. One way such anisotropy arises is that information transfer along one spatial direction is much faster than in others. In this situation, the derivative of the function is small in the local direction of a vector field $\mathbf{B}$. In order to define a discrete representation, a set of surfaces M_i indexed by an integer i are chosen such that mapping along the field $\mathbf{B}$ induces a one-to-one relation between the points on surface M_i to those on M_{i+1}. For simple cases M_i may be surfaces of constant coordinate value. On each surface M_i, a function description is constructed using basis functions defined on a regular structured mesh. The definition of each basis function is extended from the surface M along the lines of the field $\mathbf{B}$ by multiplying it by a smooth compact support function whose argument increases with distance along $\mathbf{B}$. Function values are evaluated by summing contributions associated with each surface M_i. This does not require any special connectivity of the meshes used in the neighbouring surfaces M, which substantially simplifies the meshing problem compared to attempting to find an space filling anisotropic mesh. We explore the numerical properties of the scheme, and show that it can be used to efficiently solve differential equations for certain anisotropic problems.

I. INTRODUCTION

The technique proposed here is motivated by plasma physics examples where particles travel much more easily along magnetic field lines than in the perpendicular direction, so that in quantities like fluid moments elongated structures are formed, aligned with the field lines. In particular, the technique is designed to solve problems in magnetic confinement fusion (MCF), where the field lines wind around a central axis and may be closed, trace out

surfaces, or fill ergodic regions.

A variety of techniques to deal with representing these highly anisotropic functions exist. The canonical technique is to define a 3D mesh to fill the space of interest, with the mesh strongly elongated along the field line. Achieving a very good alignment of the mesh along the field lines is in general quite a difficult meshing problem, and for this reason many MCF physics codes work only in the region where the field lines trace out a nested set of topologically toroidal magnetic surfaces: these are KAM tori[12] associated with the field line Hamiltonian. When such surfaces exist, regular grids can efficiently be generated, or angular coordinates may be employed in conjunction with a Fourier representation.

To avoid difficult meshing problems for the general case where a the region of interest is not filled by nested surfaces, it is desirable to relax the requirement of mesh connectivity. The *Flux Coordinate Independent* (FCI) approach[1, 2], based on a finite difference method, defines function values on nodes lying on a set of surfaces M_i which are taken to be surfaces of constant coordinate ζ. A node $\mathbf{r}$ on surface M_i can be mapped along the field direction $\mathbf{B}$ to find image points, $\mathbf{r}_\pm$ on surfaces $M_{i\pm1}$ Although these image points will not in general lie on nodes on the surfaces $M_{i\pm1}$, the function may be evaluated at these points by interpolation. Given the values of the function at points $\mathbf{r}_\pm$, derivatives along the field direction may then be determined.

Another way to relax the mesh connectivity constraint is via a finite volume technique, where the volumes are extrusions of a polygonal grid cell on one surface to the next, and a polynomial representation is chosen in each volume element; smoothness constraints are then approximately imposed using a discontinuous Galerkin approach.

A natural method for representing the anisotropic functions of interest is to change coordinates by defining a grid on a surface perpendicular to the mapping, and an additional coordinate along the direction of the map. Locally, this allows for straightforward and efficient representation of the problem anisotropy (as in the flux tube method[3]). However, the coordinate scheme becomes highly distorted for mappings with strong shear or compression. The mesh connectivity problem also resurfaces if the originating surface is eventually mapped back onto itself, as at this point the representation on two non-aligned meshes must be combined in some way.

We propose a partially mesh-free method for representing these anisotropic functions based on a compact-support set of basis functions which are defined in a local set of coordi-

nates aligned with the mapping; it can be thought of as a translation of the FCI method into a Galerkin approach. The definition of the set of basis functions is used to define weak forms of differential equations, as in a standard Galerkin method. The philosophy is to design a method which is robust and simple to implement, and requires little manual user interaction, because it avoids complex mesh generation tasks. The representation also provides a simple way to neatly tackle a series of related problems with slightly different configurations, generated, for example, when the field generating the mapping varies slowly with time.

II. DEFINITION OF THE FINITE DIMENSIONAL REPRESENTATION AND BASIC THEORY

For the sake of simplicity, the surfaces M of interest will be taken to be surfaces of constant coordinate ζ. Given a set of coordinates (R, Z, ζ) a point $\mathbf{r}$ may be denoted componentwise as (r_R, r_Z, r_ζ). A pair of mapping functions are defined as $\mathcal{R}(\mathbf{r}, \zeta_k)$ and $\mathcal{Z}(\mathbf{r}, \zeta_k)$, where for $\mathcal{Q} = (\mathcal{R}, \mathcal{Z}, \zeta_\parallel)$ we have the properties $\mathcal{Q}(\mathbf{r}, r_\zeta) = \mathbf{r}$ (so that the mapping is the identity where the ζ values coincide) , and

$$\frac{\partial}{\partial \epsilon} \mathcal{Q}(\mathbf{r} + \epsilon \mathbf{B}, \zeta_k) \sim 0 \tag{1}$$

so that they approximately represent the action of mapping along the field $\mathbf{B}$ from the point $\mathbf{r}$ to the point $(\mathcal{R}, \mathcal{Z}, \zeta_k)$. The geometry of this mapping is show in figure 1. The mapping is considered to be exact if it fulfils the property $\mathcal{Q}(\mathcal{Q}(\mathbf{r}, \zeta), -\zeta) = \mathbf{r}$: it then exactly maps along some field vectors $\mathbf{B}' \sim \mathbf{B}$. For consistency properties to hold, the mapping will be required to be one-to-one and at least of the same order of smoothness as the element functions defined in the next paragraph.

In the interior region the grid is defined via

$$\phi(R, Z, \zeta) = \sum_{i,j,k} \phi_{i,j,k} \tag{2}$$

$$\times \Omega_i \left[\mathcal{R}(R, Z, \zeta, \zeta_k) - R_i\right] \tag{3}$$

$$\times \Omega_j \left[\mathcal{Z}(R, Z, \zeta, \zeta_k) - Z_j\right] \tag{4}$$

$$\times \Omega_k \left[\zeta - \zeta_k\right] \tag{5}$$

with compact support basis functions Ω. We will choose the functions Ω to be B-Spline basis functions for the remainder as their properties are sufficient to ensure smoothness and

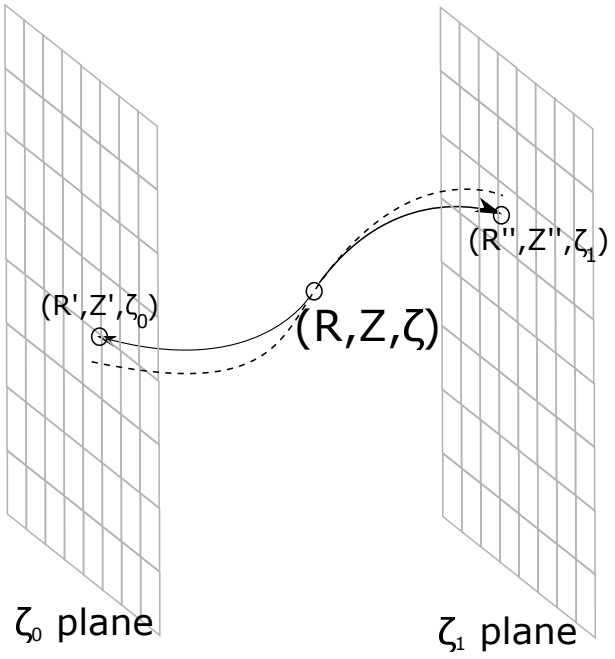

FIG. 1: The geometry of the approximate flow line mapping. Here, the mapping from the point $\mathbf{r} = (R, Z, \zeta)$ to the point (R', Z', ζ_0) on surface M_0 is depicted, with $(R', Z') = \mathbf{r}, \zeta_\prime$, as well as the analogous mapping to surface M_1. The dashed line shows the field line from the point $\mathbf{r}$, for which eq. 1 holds exactly.

lowest order consistency (and this is similar to a finite element approach used earlier in MCF codes[4, 5]). An example of the shape of a 3D basis function (the coefficient of $\phi_{i,j,k}$ for some chosen i, j and k) is given via a 2D example in figure 2. To evaluate the function value at point $\mathbf{r}$, each term of the sum in eq. 5 is evaluated by calculating the mapping $\mathcal{Q}(\mathbf{r}, \zeta_k)$, and the product of the basis functions can then be directly calculated. For a smooth mapping, the overall representation is smooth up to the order of the spline. The arguments about convergence are most simply made in the case with uniform nodes where $R_i = i\,\delta R$, $Z_j = j\,\delta Z$ and $\zeta_k = k\,\delta\zeta$. The space spanned by these functions will be denoted S.

Although it is less obvious than in a standard Finite Element formalism, these elements have a partition of unity property, and can represent the unity function exactly: setting all the coefficients equal to 1 results in an everywhere unity value. We do not, however have the δ function property that the basis function nodal values are non-zero only for the element associated with the node.

The resulting representation is smooth, and will be shown to effectively approximate

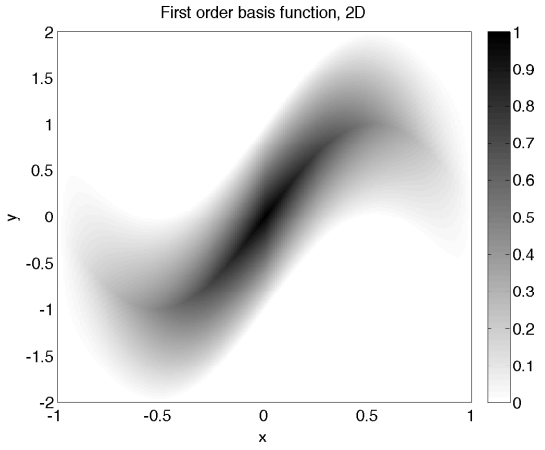

FIG. 2: A density plot of the basis function value for a 2D restriction of the method to the plane (ζ, Z). The field $\mathbf{B}$ is such that field lines are of the form $Z = \sin(\zeta/\pi) + Z_0$, and an exact mapping is used. First order B-Spline basis functions are used for Ω.

smooth functions in the large mesh resolution limit. In this paper's representation, the domains of support of basis functions associated with two nodes on different surfaces M overlap only partially, and in a potentially messy way. However, given a polynomial mapping function, the representation is piecewise polynomial within a finite set of spatial cells, where the cell faces are described by polynomial functions.

In the limit that the grid is refined isotropically in each direction, we have a parameter $h = \delta R = \delta Z = \delta\zeta$ representing the grid spacing. We wish to show that there exists $\phi \in S$ that is a good approximant to a smooth function $\bar{\phi}$ with derivatives of order 1 so that

$$\left|\phi - \bar{\phi}\right| < Ch^2. \tag{6}$$

We will need to assume a certain smoothness of the mapping function so that locally $(\mathcal{R}, \mathcal{Z}) = (R_\zeta[\zeta - \zeta_k] + R, Z_\zeta[\zeta - \zeta_k] + Z) + o(h^2)$ for constants R_ζ and Z_ζ. We will also assume that we have at least first order basis functions so that derivatives exist. A constructive proof that good approximants may be found is performed by setting the basis function

coefficients to their nodal values, so $\phi_{i,j,k} = \bar{\phi}(R_i, Z_j, \zeta_k)$. In this case we have

$$\begin{aligned}\phi = \sum_{i,j,k} \bar{\phi}(R_i, Z_j, \zeta_k) & \\ & \times\Omega\left[\mathcal{R}(R, Z, \zeta, \zeta_k) - R_i\right] \\ & \times\Omega\left[\mathcal{Z}(R, Z, \zeta, \zeta_k) - Z_j\right] \\ & \times\Omega\left[\zeta, \zeta_k\right]\end{aligned}$$

and we expand near (R_0, Z_0, ζ_0) to find

$$\begin{aligned}\phi = \sum_{i,j,k} (\bar{\phi}(R_0, Z_0, \zeta_0) + h(i,j,k).\nabla\bar{\phi}(R_0, Z_0, \zeta_0) & \\ & \times\Omega_i\left[R_\zeta(\zeta - \zeta_k) + R\right] \\ & \times\Omega_j\left[Z_\zeta(\zeta - \zeta_k) + Z\right] \\ & \times\Omega_k\left[\zeta\right] + O(h^2).\end{aligned}$$

The algebra proceeds by evaluating the j and k sums, for which ζ_k is a constant. From the definition of the derivative of B-Spline, we can show $\sum_i i\Omega_i(x) = x/h$ in the interior region. The splines also have the partition of unity property $\sum_i \Omega_i(x) = 1$ in the interior region, so the coefficient of $\bar{\phi}$ is 1, so

$$\begin{aligned}\phi = \bar{\phi} + \frac{\partial\bar{\phi}}{\partial R}\sum_k [R_\zeta(\zeta - hk) - R]\Omega_k + \frac{\partial\bar{\phi}}{\partial Z}\sum_k [Z_\zeta(\zeta - hk) - Z]\Omega_k + \frac{\partial\bar{\phi}}{\partial\zeta}\sum_k k\Omega_k + O(h^2) & \\ = \bar{\phi} + (R, Z, \zeta).\nabla\bar{\phi} + O(h^2) &\end{aligned}$$

and from the smoothness of ϕ we have $\phi = \bar{\phi} + O(h^2)$ in the vicinity of any grid point. Similarly, we can show that the error in derivatives is $O(h)$.

However, better bounds are expected in practice due to an equivalence with more standard discretisations. For an exact mapping, it is useful to view the discretisation in a 'flux tube' type coordinate scheme $(R', Z', \zeta) = (\mathcal{R}[\mathbf{r}, \zeta_0], \mathcal{Z}[\mathbf{r}, \zeta_0], \mathbf{r}_\zeta)$. The representation on each surface M_i in these coordinates with $i \neq 0$ is smoothly distorted by the mapping function, which varies on system scale lengths, so the representational power for smooth functions is equivalent to the undistorted mapping: we expect it to be consistent to the same order as the original mapping. The overall representation is then a tensor product of spline functions

along the ζ direction with these nth order consistent representations based on surface M_i. At lowest order, the distortion is just a translation in $\mathcal{Q}$ in which case polynomials of order n are exactly represented on each plane M_i. For somewhat inexact mappings, we may lose some accuracy of approximation, but this effect has not been investigated in detail.

Various functional equations for spatial unknowns (typically differential and integro-differential equations) may be represented in this method via their weak form. For an equation $A(\phi) = 0$, we require that the discrete representation ϕ, for all weight functions ψ in the reduced function space, satisfies

$$\int \psi A(\phi) = 0. \tag{7}$$

Where A is a local function of ϕ (usually a differential operator) the integration involves evaluations of ϕ and ψ at the same spatial locations, and in the standard finite element formalism, the spatial mesh of elements forms a natural basis for a quadrature (integration) mesh; for polynomial basis elements, appropriate quadratures (such as Gauss points) are well-known, which allow machine-precision evaluation of these integrals at reasonable cost. In general mesh-free methods, the lack of alignment between the basis function support domains means that the favourable convergence properties of Gauss quadrature cannot generally be expected[6].

In the set of coordinates $(\mathcal{R}, \mathcal{Z}, \zeta)$, with an invertible mapping, the piecewise polynomial domains of integration are given the tensor product of areas I in the $(\mathcal{R}, \mathcal{Z})$ plane multiplied by intervals in ζ. The areas are bounded by curves which lie on the union of the images of the meshes of nearby mother planes. For practical examples the boundaries of these areas are approximately polygonal, with low curvature edges. Calculation of these intersections can be performed with standard packages at least where edges can be taken to be straight. Boundary conditions will complicate the meshing process substantially. We will avoid finding such meshings in this paper, as the motivation of the method is precisely to avoid complex mesh generation.

Increasing the number of Gauss points over that required for a standard mesh problem has been found to be sufficient in tests of certain mesh-free methods[7]. Depending on the problem of interest, a brute-force equidistant equal-weighted integration scheme may be of sufficient accuracy. We are frequently interested in cases where the operator A is non-local, so that evaluation points of ϕ and ψ are different[8, 9] and the usual quadrature

approaches are not well-justified. The quadrature is specified on a mesh which conforms to the boundaries[7], this is only straightforward if the geometry of the boundaries is relatively simple.

Boundary conditions may be handled in a FEM by generating a mesh that conforms to the boundary surface, and ensuring the finite element basis functions are consistent with the boundary conditions. The mesh volumes are strongly curved along the ζ direction, so even if the boundary is flat in Cartesian coordinates, it is curved in the natural mesh coordinates. This leads to a somewhat messy meshing problem, as in general volumes need to be broken into smaller pieces to approximate the curves with flat faces. An additional coordinate transform can be used to map the curved surfaces to flat faces via an isoparametric transform but this will still require some mesh realignment.

There are a number of approaches to handling boundaries in mesh-free methods[10, 11]. In the methods close in spirit to that proposed here, essential boundary conditions can be imposed by transforming shape functions so that they conform, by introducing penalty functions to the minimisation problem resulting from the weak form, or by introducing an additional boundary mesh that conforms exactly. We will use the latter method, where a standard finite element method mesh is defined near the boundary: this may be a sizeable number of additional nodes for very anisotropic methods.

III. AN EXAMPLE PROBLEM

The motivating problem is magnetic confinement fusion, where a plasma is confined by a magnetic field, generated by external and internal currents. Plasma is free to stream rapidly along field lines, but well confined regions of plasma can still exist because in a substantial volume of vacuum vessel the field lines lie on a nested set of flux surfaces which are topologically toroidal (nested KAM tori[12]). Consider the field lines shown in fig. 3: if the bounding rectangle is taken to be a physical wall, the volume can be separated into an 'open field line' region, whose magnetic field lines intersect the wall, and a closed field line region. Fig. 3 is typical of a 'diverted' tokamak configuration, where the nested set of flux surfaces end at a separatrix, and points outside the last closed flux surface are connected by the magnetic field lines to the wall.

A common computational task is to trace the trajectories of particles in a turbulent

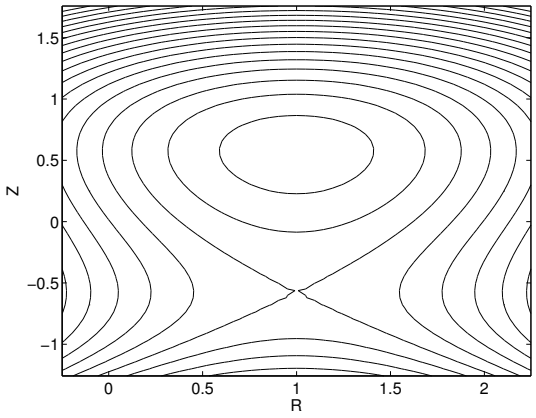

FIG. 3: Countours of the function A specified in equation 9. These contours are the projections of $\mathbf{B}$ field lines onto the (R, Z) plane.

field generated by some set of charges and currents, which may be part of a particle-in-cell simulation[5, 13]. Accuracy of particle tracing requires a smooth representation of the fields, and a partial differential equation (in general integro-differential) must be solved to determine the fields based on currents and charge sources; we will explain how to use the partially mesh free method to solve an example problem of this type.

We define a magnetic field

$$\mathbf{B} = B_0 \boldsymbol{\zeta} + \boldsymbol{\zeta} \times \nabla A(R, Z) \tag{8}$$

with

$$A(R, Z) = (R - 1)^2 + Z(Z^2 - 1) \tag{9}$$

which represents a diverted configuration in the large aspect ratio limit. The contours of A (figure 3) are the field lines projected onto the (R, Z) plane, and a separatrix is seen at $(R, Z) = (0, -1/\sqrt{3})$.

The differential equation we choose here (typical for the problems of electromagnetic coupling which arise in tokamak turbulence) is the Laplacian inverse over a rectangular domain in R, Z and a periodic ζ direction:

$$\nabla^2 \phi = \rho \tag{10}$$

with $\phi = 0$ on the boundaries of the domain. We take $R \in [R_0, R_1]$ and $Z \in [Z_0, Z_1]$ and $\zeta \in [0, \zeta_1]$. In order to ensure that the representation satisfies the boundary conditions

exactly, we use a single cell-width first order standard FEM formalism near the boundary, blended with the FCIFEM method using a ramp function.

Second-order B-Splines basis functions are chosen to represent the field, with uniform grid spacing δR, δZ, $\delta\zeta$.

Discretisation proceeds by taking the weak form and finding $\phi \in S$ such that

$$\int dV(\nabla\psi.\nabla\phi + \psi\rho) = 0 \tag{11}$$

for all $\psi \in S$. The integration is performed using a set of quadrature points evenly spaced in R, Z and ζ, 10 times finer than δR, δZ, $\delta\zeta$ respectively.

In order to examine the basic convergence of the method, a simple test problem is considered with $\rho(R) = \sin(0.5\pi R)\sin(\pi[Z + 1.0]/2.5)$. the domain $R_0 = 0$, $R_1 = 2$, $Z_0 = -1$, $Z_1 = 1.5$ and $\zeta_1 = \pi/20$ is chosen. The solution ϕ to this test-problem is not aligned along the field, but constant along ζ, so the use of the FCIFEM is not advantageous in this case. Along the field line, the perturbation varies with typical scale length $|B_\zeta|/|B_{R,Z}|$ times longer than typical wavelengths in R and Z. We have therefore chosen δZ comparable to $\delta R|B_\zeta|/|B_{R,Z}|$ so that the effective resolution is sufficiently high along the field line.

The field-aligned mesh leads to projected domains of the basis functions in the (R, Z) plane of extent $\sim |\mathcal{Q}[R, Z, \delta\zeta] - \mathcal{Q}[R, Z, 0]| + |\delta R| + |\delta Z|$, so the effective reso

The number of grid points at lowest resolution $(N_R, N_Z, N_\zeta) = (20, 20, 1)$, and this is uniformly increased by a factor H in each direction to perform a convergence scan (the convergence in N_ζ is not trivial because the element connectivity changes with N_ζ). Figure 4 shows the L^2 error ϵ in the solution versus H, which drops as $H^{3.2}$, in line with the value 3 expected for a standard second order FEM, and as good as could be expected for the degree of representation smoothness chosen.

In order to illustrate the treatment of anisotropic structures in this method, we consider a second test problem in the same spatial domain as the previous problem. Here, we take $\rho(R) = \int d\zeta[\delta(\mathbf{R}\mathbf{r}(\zeta)) - \delta(\mathbf{R} - \mathbf{r}(\zeta) - \hat{\zeta}\zeta_1/2)]$ with $\mathbf{r}(\zeta)$ the curve traced out by a field line parameterised by ζ, starting from the point $\mathbf{r}(0) = (0.6, 0.2, 0)$, so that it passes near the separatrix. This results in a highly anisotropic charge perturbation along the magnetic field lines with neighbouring charge filaments of opposite sign, typical of a localised unstable drift mode. The number of grid points in each direction is $(N_R, N_Z, N_\zeta) = (100, 100, 1)$; because the perturbation is highly field aligned, the solution is expected to be also well-aligned, so

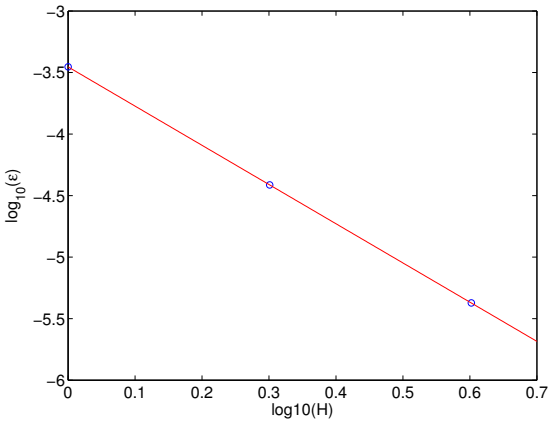

FIG. 4: Convergence of the L^2 error for a simple analytical test problem in a rectangular domain with the FCIFEM method and a mapping function based on a divertor-type field.

that the anisotropic solution is well captured, despite using only 1 point in the ζ direction.

The resulting matrix problem, coupling the coefficients of the ϕ representation to those of the weight function, is a sparse matrix of rank equal to the number of degrees of freedom of the system, which we treat as being unstructured. Index reordering is quite effective in reducing the bandwidth of the resulting matrix, so that direct solution using banded matrix calculation is straightforward for the test problem under consideration.

To show the projection of the charge ρ into the space S, the weak form

$$\int dV(\psi.\bar{\rho} - \psi\rho) = 0 \tag{12}$$

is solved for $\bar{\rho} \in S$ by finding and inverting the *mass matrix*. We show 2D plots and 3D plots of $\bar{\rho}$ and ϕ in figure 5. Due to the structure of the charge (alternating charge lines of opposite sign), the potential ϕ decays rapidly away from the field lines where ρ is nonzero. The strong anisotropy of the charge and of ϕ are clear in the 3D plots: a conventional Cartesian grid would need of order 20 grid points in the ζ direction Near the separatix (X-point) the spacing between charge lines become too fine for the grid to resolve. Behaviour near the boundaries is acceptable from visual inspection in the reproduced field and the solution to the Laplacian problem.

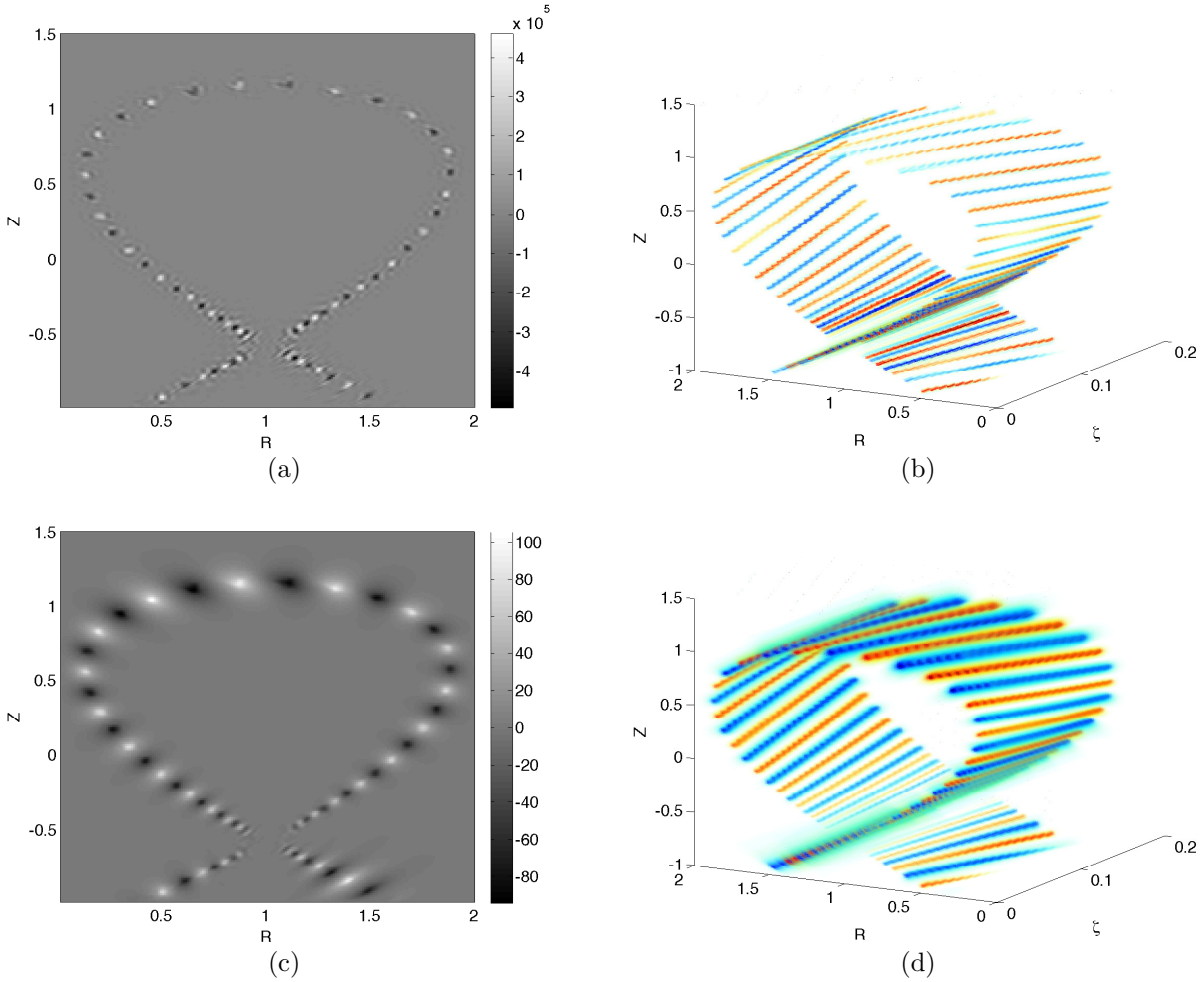

FIG. 5: 2D plots versus R and Z at $\zeta = 0$ (a,c), and 3d voxel renderings (b,d), of $\bar{\rho}$ (a,b) and ϕ (c,d). 2D plots evaluate the functions at doubled grid resolution in R, Z. 3D plots use 20 samples in ζ for rendering purposes, and show regions of positive charge/potential as red, and negative as blue. The ζ direction extends periodically with period $\pi/20$, but repeats are not shown.

Acknowledgments

This work has been carried out within the framework of the EUROfusion Consortium and has received funding from the Euratom research and training programme 2014-2018 under grant agreement No 633053. The views and opinions expressed herein do not necessarily

reflect those of the European Commission.

---

[1] F. Hariri and M. Ottaviani, Computer Physics Communications **184**, 2419 (2013), ISSN 0010-4655.

[2] M. Ottaviani, Physics Letters A **375**, 1677 (2011), ISSN 0375-9601.

[3] M. A. Beer, S. C. Cowley, and G. W. Hammett, Physics of Plasmas **2**, 2687 (1995).

[4] M. Fivaz, S. Brunner, G. de Ridder, O. Sauter, T. Tran, J. Vaclavik, L. Villard, and K. Appert, Computer Physics Communications **111**, 27 (1998), ISSN 0010-4655.

[5] S. Jolliet, A. Bottino, P. Angelino, R. Hatzky, T. Tran, B. McMillan, O. Sauter, K. Appert, Y. Idomura, and L. Villard, Computer Physics Communications **177**, 409 (2007).

[6] J. Dolbow and T. Belytschko, Computational Mechanics **23**, 219 (1999), ISSN 0178-7675.

[7] T. Belytschko, Y. Krongauz, D. Organ, M. Fleming, and P. Krysl, Computer Methods in Applied Mechanics and Engineering **139**, 3 (1996), ISSN 0045-7825.

[8] J. Dominski, S. Brunner, B. McMillan, T.-M. Tran, and L. Villard, Transport Task Force Meeting, San Antonio Texas (2014).

[9] A. Mishchenko, A. Knies, and R. Hatzky, Physics of Plasmas **12**, 062305 (2005).

[10] P.-H. Chavanis, Physica D: Nonlinear Phenomena **200**, 257 (2005), ISSN 0167-2789.

[11] A. Huerta, S. Fernndez-Mndez, and W. K. Liu, Computer Methods in Applied Mechanics and Engineering **193**, 1105 (2004), ISSN 0045-7825, meshfree Methods: Recent Advances and New Applications.

[12] A. N. Kolmogorov, Dokl. Akad. Nauk SSSR **98**, 527 (1954).

[13] C. Birdsall and A. Langdon, *Plasma physics via computer simulation* (New York, Taylor and Francis, 1985).